Simplified Method for the Characterization of the Hydrograph following a Sudden Partial Dam Break

Marco Pilotti[1]; Massimo Tomirotti[2]; Giulia Valerio[3]; and Baldassare Bacchi[4]

Abstract: This paper presents a simplified approach to the characterization of the hydrograph following the partial collapse of concrete gravity dams. The proposed approach uses a simplified representation of the reservoir geometry and is based on the numerical solution of shallow water equations to study the two-dimensional evolution of the water surface within the reservoir. The numerical results are made dimensionless and reorganized so as to compute the peak discharge, the duration and the recession limb of the dam break hydrograph. The proposed practical approach provides a quite satisfactory reproduction of the computed hydrograph for a wide set of realistic situations that have been simulated in detail.

DOI: 10.1061/(ASCE)HY.1943-7900.0000231

CE Database subject headings: Dam failure; Shallow water; Numerical models; Simulation; Outflow; Hydrographs.

Author keywords: Dam failure; Dam breaches; Shallow water; Numerical simulation; Outflow.

Introduction

According to research on dam safety worldwide (Goubet 1979), the overall yearly probability of dam failure can be reckoned around 1/50,000, so that the a priori probability of failure during the lifetime of a dam, supposedly equal to 100 years, can be estimated between 10^{-2} and 10^{-3}. Anyway, the potential consequences of this type of accident are so severe that every effort must be made in order to reduce them further and to forecast, in a better way, the expected flood extent and effect in the tailwater areas. In order to cope with these important issues, most national legislations prescribe dam safety regulations regarding not only the construction and upgrading of dams but also their operation and maintenance and emergency preparedness plans, so as to minimize the potential harm to the public and damage to property. In this direction, it is of primary importance to take into account the conceivable failure scenarios applicable to the dam in order to compute a realistic flood wave at the dam site that can be routed downstream to outline and characterize the inundated area. The two primary tasks in the hydraulic analysis of a dam break are the prediction of the reservoir outflow hydrograph and the routing of this boundary condition through the tailwater areas. In this paper we will restrict our attention to the first problem for nonerodible dams.

The problem of the computation of the hydrograph following the collapse of a dam has been a major concern since the end of 19th century. Whilst the first documented experimental dam break case in a channel was probably investigated by Bazin (1865), Ritter (1892) derived an analytical solution of the one-dimensional (1D) De Saint Venant equations for the case of instantaneous removal of a barrage retaining a reservoir in a frictionless, initially dry, horizontal channel with rectangular cross section. Su and Barnes (1970) extended Ritter's solution considering the effects of different channel cross-sectional shapes. The power-type expression that they introduced for the wetted area, depending on the value of an exponent, is suitable to represent cross sections varying from rectangular to parabolic and triangular shapes. To the writers knowledge, very few works proposing new analytic advancement to this problem have been presented afterwards (e.g., Sakkas and Strelkoff 1973; Wu et al. 1999). On the other hand, significant advances have been made in the numerical solution of De Saint Venant equations. Several papers have dealt with the detailed reconstruction of floods following important dam failures, such as the Malpasset dam break (e.g., Valiani et al. 2002), the Gleno dam break (Pilotti et al. 2006), and the Saint Francis dam break (e.g., Begnudelli and Sanders 2007). These modelling efforts show that, albeit under the hydrostatic assumption, it is possible to provide a detailed and reliable description of the hydrograph formation and propagation.

The analytic solutions that have been mentioned (Ritter 1892; Su and Barnes 1970) have limited practical scope for the evaluation of the hydrograph at the breach section. These solutions assume an infinitely long reservoir with the consequence that the discharge at the breach is constant in time. On the other hand, the two-dimensional (2D) numerical simulation of a dam break case always requires a great deal of information (e.g., the reservoir bathymetry) and a considerable level of expertise. Often in practical applications both these requirements cannot be satisfied.

These considerations have motivated the introduction of sim-

[1]Associate Professor, Dipartimento di Ingegneria Civile, Architettura, Territorio e Ambiente—DICATA, Università degli Studi di Brescia, Via Branze 43, 25123 Brescia, Italy (corresponding author). E-mail: marco.pilotti@ing.unibs.it

[2]Associate Professor, Dipartimento di Ingegneria Civile, Architettura, Territorio e Ambiente—DICATA, Università degli Studi di Brescia, Via Branze 43, 25123 Brescia, Italy. E-mail: massimo.tomirotti@ing.unibs.it

[3]Ph.D. Student, Dipartimento di Ingegneria Civile, Architettura, Territorio e Ambiente—DICATA, Università degli Studi di Brescia, Via Branze 43, 25123 Brescia, Italy. E-mail: giulia.valerio@ing.unibs.it

[4]Full Professor, Dipartimento di Ingegneria Civile, Architettura, Territorio e Ambiente—DICATA, Università degli Studi di Brescia, Via Branze 43, 25123 Brescia, Italy. E-mail: bacchi@ing.unibs.it

Note. This manuscript was submitted on December 25, 2008; approved on March 23, 2010; published online on March 27, 2010. Discussion period open until March 1, 2011; separate discussions must be submitted for individual papers. This paper is part of the ***Journal of Hydraulic Engineering***, Vol. 136, No. 10, October 1, 2010. ©ASCE, ISSN 0733-9429/2010/10-693–704/$25.00.

plified methodologies to deal with the problem of the breach-outflow hydrograph characterization following a sudden dam break. Usually, these methodologies couple a steady-state weir-like relationship for the discharge to the continuity equation for the volume of the reservoir and so neglect the role of inertial terms on the outflow process, possibly overpredicting considerably the outflow peak (e.g., Aureli et al. 2007). Actually, in the real dam break problem, part of the initial potential energy stored in the head difference is transferred upstream in the negative wave that accelerates water in the reservoir. Sometimes the breach-outflow hydrograph is approximated as a triangle, where the base represents the emptying time of the reservoir and the height is estimated from the instantaneous peak outflow (e.g., Owen 1980) evaluated, e.g., by Ritter's equation, often applied under the simplified hypothesis of rectangular section.

Aureli et al. (2007) have recently proposed a simple procedure that parameterizes the breach hydrograph on the basis of a numerical solution of the dimensionless 1D De Saint Venant equations, in the case of a frictionless sloping bed with a cross section shape described according to Su and Barnes' geometry. This procedure satisfies the constraint on the volume actually stored within the reservoir and requires input data usually available for most man-made storages.

All these researches have assumed a total and sudden dam break. Although there is general agreement that the latter hypothesis is a good approximation to a process that usually evolves very rapidly, there is clear evidence that for several types of dams the failure can be, and usually is, partial. This is true for gravity dams, when their stability is verified independently for each vertical monolith. In these situations, assuming a total dam break would result in an unrealistically high flood wave and therefore the breach size is normally assumed to cover a multiple of monolith widths [e.g., Owen 1980; ICOLD 1998; U.S. Army Corps of Engineers (USACE) 1997]. Accordingly, the dam safety regulations of several nations introduce the possibility that the reservoir outflow hydrograph can be computed under the assumption of partial dam break. This is the case, e.g., for Italian regulation, where for certain types of dam the breach can be partial, but must involve the highest elements of the structure with a minimum breach area $a \geq 0.3\,A_0$, being A_0 the total initially wetted area of the dam.

On the other hand, partial dam break has a peculiarity of its own: it can be shown that the peak discharge in a partial dam break is higher than that obtainable by using the Ritter equation, although modified to take into account the actual shape of the lower arch of the valley (e.g., Bukreev 2006).

In spite of the importance of this topic, to our knowledge, no satisfactory simplified procedure has been so far specifically developed for partial dam break hydrograph estimation. In order to contribute to fill this gap, in this paper we study the emptying process of partially breached reservoirs characterized by a cross section whose geometry is based on Su and Barnes' assumptions and whose thalweg is uniformly inclined. The potential field of variation of the parameters for this geometry has been identified through the inspection of a wide range of different real site conditions. The analysis of an extensive set of outflow hydrographs obtained through numerical solution of the 2D De Saint Venant equations on the basis of a dimensional analysis of the process, suggests that they depend primarily on a limited number of nondimensional groups. This permits the expression of the discharge hydrographs in a simplified fashion, while retaining the most significant aspects of the process. By considering a wide set of real bathymetries located in mountain areas, we show that the identified functional dependence can be easily applied also to several real situations by a simple procedure that requires data usually available for most man-made reservoirs. When the valley geometry is well represented by the hypotheses which are placed at the basis of this proposal, the comparison of the synthetic hydrographs, obtained through the application of the simplified procedure presented in this paper, with the numerically computed ones, shows a very satisfactory agreement.

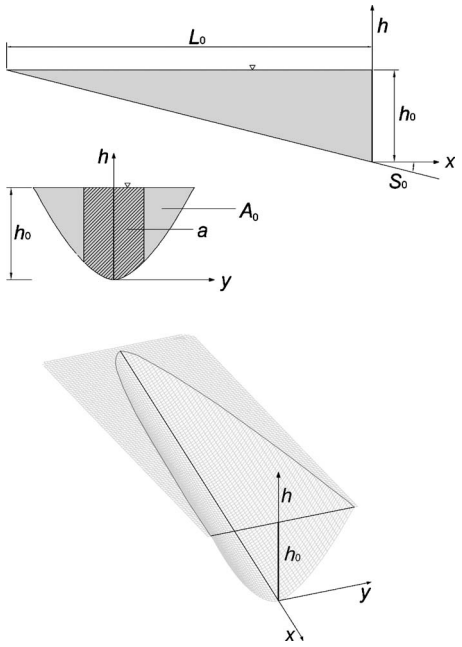

Fig. 1. Schematic reservoir bathymetry adopted in this paper (here $\lambda = 1.6$)

Dimensionless Expression of the Hydrograph Following a Sudden Partial Dam Break

The outflow hydrograph, due to the reservoir emptying following a sudden dam break, has a shape that depends on the reservoir bathymetry and on the breach geometry. These quantities determine both the overall volume and the discharge time evolution, particularly during the initial phase of the process. In order to derive a methodology that is as simple as possible, without losing effectiveness, the valley geometry where the dam is located is described as prismatic having a cross section area A represented by a power-type expression (Su and Barnes 1970)

$$A = \delta h^{\lambda} \tag{1}$$

where h=depth; and δ and λ=parameters which depend on the cross-sectional shape. In addition, the valley longitudinal axis should have a constant slope, as shown in Fig. 1. Although not exhaustive, the type of geometric representation provided by Eq. (1) is particularly effective in representing the "U" or "V" shaped cross sections of glacial or fluvial mountain valleys because the cross section shape can be changed continuously with λ from rectangular ($\lambda = 1$) to parabolic ($\lambda = 1.5$) and triangular ($\lambda = 2$; see Fig. 2). Although simplified, this scheme seems suitable to interpret the bathymetry of a large variety of mountain reservoirs, as will be shown in the final part of this contribution. For a reservoir described by Eq. (1) and whose thalweg has a slope $S_0 = h_0 / L_0$, where h_0=initial water depth in the reservoir at

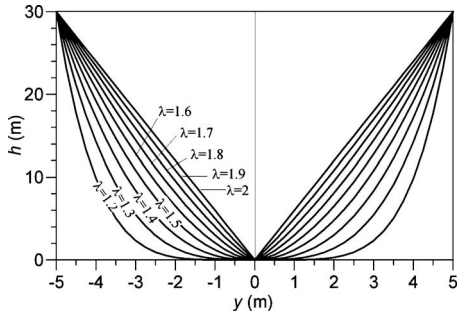

Fig. 2. Shape of a reservoir cross section for λ in the range of 1.2–2

the dam location; and L_0=initial extent of the water surface, measured orthogonally to the dam (see Fig. 1), consider a partial collapse in an initially dry and infinitely long valley as a consequence of the sudden removal of the central stripe of area a, taken symmetrically with respect to the vertical symmetry plane of the reservoir. If inviscid conditions are assumed, the resulting hydrograph at the breach can be described as a function of several independent dimensional quantities

$$Q = f(t, \delta, \lambda, L_0, h_0, a, g) \tag{2}$$

where, in addition to the dependence on time t, the other characteristic parameters express the dependence on

1. Valley shape: δ, λ, h_0/L_0;
2. Initial water depth: h_0;
3. Shape and extension of the breach: a, in addition to the above mentioned δ and λ that describe the lower arch of the breach; and
4. The acceleration due to gravity, g.

These parameters are mutually independent and are necessary and sufficient for a complete definition of the phenomenon.

Eq. (2) can be rewritten in a dimensionless form. According to the Π-theorem, choosing h_0 and g as basic quantities, one can write a dimensionless expression Π_1 of the discharge Q, as

$$\Pi_1 \equiv \frac{Q}{\delta h_0^{\lambda}\sqrt{g h_0}}\sqrt{\lambda}\left(\frac{2\lambda+1}{2\lambda}\right)^{2\lambda+1} = f\left(\frac{a}{\delta h_0^{\lambda}}, \frac{L_0}{h_0}, \lambda, \frac{\delta}{h_0^{2-\lambda}}, t\sqrt{\frac{g}{h_0\lambda}}\frac{h_0}{L_0}\right)$$
$$= f(\Pi_2, \Pi_3, \Pi_4, \Pi_5, \Pi_6) \tag{3}$$

Similar relationships can be written with reference to any other dimensional property of the process, where the form of the function f will depend upon the nature of the property under investigation. This conclusion obviously does not imply that f must necessarily depend on all five of the dimensionless groups on the right side. With respect to a particular property, they have to be regarded merely as sufficient. As an example, if one considers the dimensionless expression of the peak discharge Q_p, it clearly does not depend on Π_6.

The dimensionless expression Π_1 of the discharge Q in Eq. (3) has been obtained by using the theoretical generalization of Ritter's solution for the discharge at the breach in the case of a total collapse of the dam (Π_2=1) and horizontal infinitely long bed (Π_3=∞) provided by Su and Barnes (1970)

$$\frac{Q}{\delta h_0^{\lambda}\sqrt{g h_0}}\sqrt{\lambda} = \left(\frac{2\lambda}{2\lambda+1}\right)^{2\lambda+1} \tag{4}$$

This equation is valid for t=0 also in the case of sloping bed. However, the discharge is constant in time when the bed is horizontal whilst it decreases if the slope is different from zero.

Π_2 reflects the role of the breach area with respect to the overall initial cross section, given by Eq. (1). In the same way, if one considers that in the geometry under consideration the celerity of a long wave of small amplitude, c, is given by

$$c(h) = \sqrt{g\frac{A(h)}{B(h)}} = \sqrt{g\frac{\delta h^{\lambda}}{\lambda\delta h^{\lambda-1}}} = \sqrt{g\frac{h}{\lambda}} \tag{5}$$

being $B(h)$=free surface width in correspondence of depth h; then Π_6 provides a significant dimensionless time including the ratio between the reservoir length, L_0, and the initial celerity at the breach, c_0.

As will be shown in the following, a better standardization of the discharge is empirically obtained if one considers the dimensionless discharge in the form:

$$\Pi_7 \equiv \frac{Q}{\delta h_0^{\lambda}\sqrt{g h_0}}\left(\sqrt{\lambda}\left(\frac{2\lambda+1}{2\lambda}\right)^{2\lambda+1}\right)^{a/A_0} \tag{6}$$

Accordingly, one can write a symbolic relationship for the dimensionless hydrograph at the breach, which is conceptually equivalent to Eq. (3)

$$\frac{Q}{\delta h_0^{\lambda}\sqrt{g h_0}}\left(\sqrt{\lambda}\left(\frac{2\lambda+1}{2\lambda}\right)^{2\lambda+1}\right)^{a/A_0} = f\left(\frac{a}{\delta h_0^{\lambda}}, \frac{L_0}{h_0}, \lambda, \frac{\delta}{h_0^{2-\lambda}}, t\sqrt{\frac{g}{h_0\lambda}}\frac{h_0}{L_0}\right) \tag{7}$$

In the following, Eq. (7) has been simplified to limit the degrees of freedom of the model. To this purpose, it is relevant to observe that each dimensionless group reflects mostly the influence of the characteristic parameter that appears only within it. Accordingly, the breach area and the cross section shape are basically described by Π_2 and by Π_4. The other shape parameter, δ, appears within Π_5 but, indirectly, also in Π_2 and Π_7.

Moreover, from the Su and Barnes' solution Eq. (4), in the case of total collapse the discharge at the dam location is independent of Π_5, being the influence of δ on the process described by the expression of the dimensionless discharge. Accordingly, it seems reasonable to make the hypothesis that Π_5 plays a negligible role also for a partial dam break.

In the same way, L_0 appears directly in Π_3 but also within Π_6. If all other variables are kept constant, L_0 mostly influences the wave peak and the emptying time. However, when L_0/h_0 is not small, the influence on the wave peak tends to disappear because this is influenced by the area surrounding the breach, which is only marginally affected by the valley slope. This is also confirmed by the theoretical results by Dressler (1958) who studied the instantaneous and complete removal of a dam on a sloping channel of infinite width, showing that the dimensionless hydrograph does not depend on Π_3. In conclusion, it seems possible to make the hypothesis that the direct dependence of Eq. (7) on the group Π_3 can be disregarded.

Under the abovementioned assumptions it is possible to simplify the dimensionless relationship Eq. (7) as

$$\frac{Q}{\delta h_0^{\lambda}\sqrt{g h_0}}\left(\sqrt{\lambda}\left(\frac{2\lambda+1}{2\lambda}\right)^{2\lambda+1}\right)^{a/A_0} = f\left(\frac{a}{\delta h_0^{\lambda}}, \lambda, t\sqrt{\frac{g}{h_0\lambda}}\frac{h_0}{L_0}\right) \tag{8}$$

that provides a direct dependence of the dimensionless flood wave following a sudden partial dam break on the dimensionless time, when λ and the breach ratio a/A_0 are kept constant.

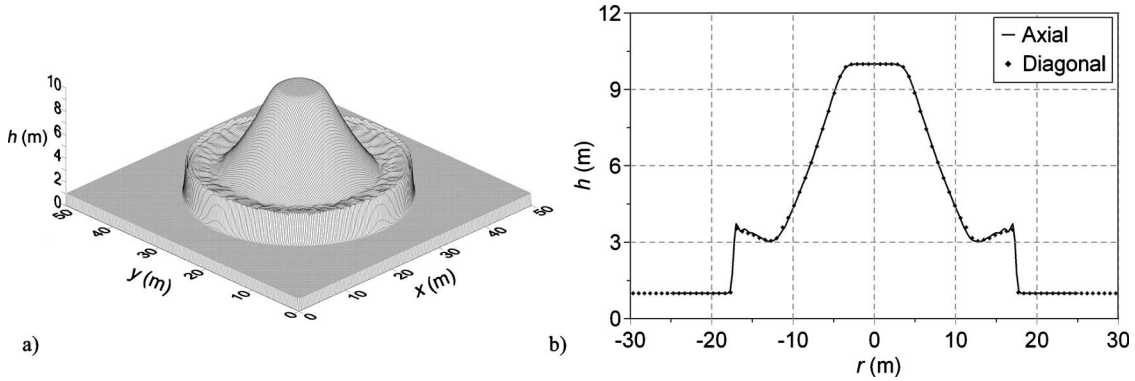

Fig. 3. (a) Surface plot of circular dam break (initial water height is 10 m inside dam and 1 m outside; dam radius is 11 m and cell side is 0.25 m; (b) comparison between profiles for $t=0.693$ s

Numerical Simulation of Reservoir Emptying Process

In order to verify the validity and scope of Eq. (8), we have made a careful comparison with the results of detailed numerical simulations. To this purpose we have studied the emptying process of many reservoirs whose bathymetry is described by Eq. (1), when the dam bounding the reservoir is suddenly removed to form a breach as shown in Fig. 1. Although the outflow process following a dam break presents strongly three-dimensional (3D) features in the neighbourhood of the breach, a useful and effective approximation of the process is obtained by using 2D De Saint Venant equations, according to the assumption of the hydrostatic pressure distribution in the vertical. Disregarding Coriolis and wind forces, the shallow water equations (SWEs) can be written in a conservative vectorial form as

$$U_t + E_x + F_y + S = 0 \tag{9}$$

where subscripts denote partial derivatives, being

$$U = \begin{pmatrix} h \\ uh \\ vh \end{pmatrix};\quad E = \begin{pmatrix} uh \\ u^2h + \frac{1}{2}gh^2 \\ uvh \end{pmatrix};\quad F = \begin{pmatrix} vh \\ uvh \\ v^2h + \frac{1}{2}gh^2 \end{pmatrix}$$

$$S = \begin{pmatrix} 0 \\ -gh(S_{0x} - S_{fx}) \\ -gh(S_{0y} - S_{fy}) \end{pmatrix} \tag{10}$$

$$S_{0x} = -\frac{\partial z}{\partial x};\quad S_{0y} = -\frac{\partial z}{\partial y};\quad S_{fx} = \frac{u\sqrt{u^2+v^2}}{\chi^2 h};\quad S_{fy} = \frac{v\sqrt{u^2+v^2}}{\chi^2 h} \tag{11}$$

where x, y=orthogonal space coordinates on a horizontal plane and t is the time; u, v=velocity components along x- and y-directions; and S_{0x} and S_{0y} the bottom slope, S_{fx} and S_{fy} the slope friction along the same directions. The Chezy's coefficient χ can be computed using Manning's roughness coefficient.

In order to solve Eq. (9), a solver has been implemented based on the well known MacCormack finite difference scheme (Fennema and Chaudhry 1990). This solver has been carefully validated using the available classic test cases (e.g., Ritter's and Stoker's cases, steady flow through a sequence of a contraction expansion and on a bump, circular dam break, etc.), always obtaining very satisfactory results. As an example of a 2D test case, in Fig. 3(a) we show the results obtained in the case of a radially symmetric dam break centered in a square initially wet domain (Alcrudo and Garcia Navarro 1993). Fig. 3(b) shows the comparison between axis and diagonal profiles of the computed water surface; as one can observe, the circular symmetry is preserved very well and shocks are well resolved.

In view of its application presented in the following section, it might be interesting to validate the numerical code also with respect to some laboratory experiments regarding dam break in sloping channels. In the following, we have considered the set of experiments accomplished by the U.S. Army Corps of Engineers Waterways Experiment Station (WES) (1960) in conditions of minimum resistance. This set of experiments is particularly interesting because it regards both complete and partial dam break. The experiments were accomplished in a wooden rectangular flume, with Manning's n equal to 0.009 $s/m^{1/3}$. The flume is 4 ft wide and 400 ft long and is constructed on a slope equal to 0.005 ft/ft, with the dam located midway of its length. The dam was suddenly removed at time zero, with an initial water level at the upstream side of 1 ft. Observations regarding stage-time hydrographs were made both upstream and downstream of the dam, so providing experimental information on the reservoir emptying process that can be numerically reproduced. In this simulation as well as in all the following dam break cases, we have adopted a downstream far-field boundary condition, according to which the gradient of conserved quantities is set to zero. A free slip condition has been applied along solid walls, setting to zero the normal flow velocity component.

Due to space constraints, here we limit our attention to experiment 3.1 of WES, characterized by initial dry bed condition and full depth breach with ratio $a/A_0=0.3$, close to the lowest value admitted in dam break studies by some national regulations. Fig. 4 shows a comparison between measured and computed stage-time hydrographs within the reservoir at distance 40, 120, 172, and 199 ft from upstream. Since the experimental depths published by WES were obtained by averaging across each section, the same procedure was adopted for our numerical results. Fig. 5 shows a comparison between experimental and numerical discharge hydrographs at the breach. As one can observe, there is a satisfactory agreement between experimental data and numerical results. However, a difference is noticeable in the first 40 seconds, where the experimental hydrograph is characterized by an almost steady discharge, while the numerical hydrograph shows a decreasing pattern, as one could expect considering the theoretical solution provided by Dressler (1958) for the case of

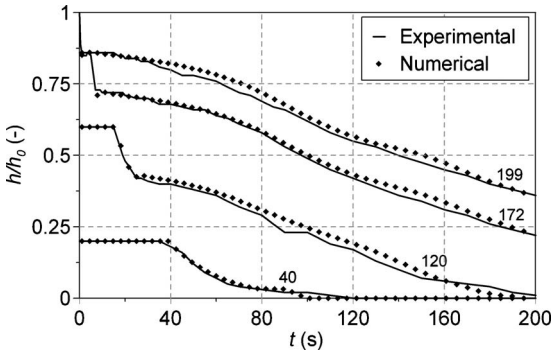

Fig. 4. Measured (WES) and computed stage-time hydrographs within the reservoir at four different distances (in feet) from upstream; h_0 is the initial stage at the breach

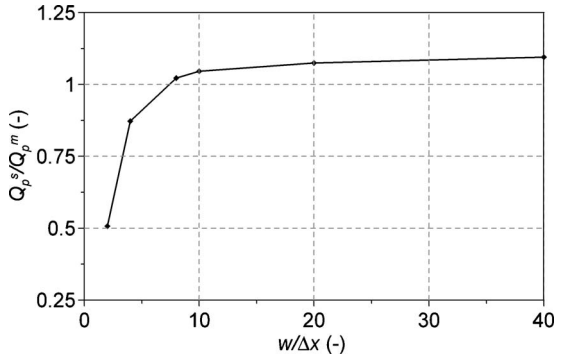

Fig. 6. Peak discharge for MacCormack 2D simulations (Q_p^s) as a function of the number of cells on the breach. Q_p^m is the measured (WES) peak discharge and w is the width of the breach.

total dam break in a sloping channel. Here one must observe that the experimental hydrograph has been obtained by WES through numerical differentiation of a cumulative "volume of outflow as a function of time" curve, computed using measured stage data (Table 3 of WES 1960). By repeating the same procedure one can observe that in reality the initial part of the discharge hydrograph is uncertain because extremely sensitive to the type of differentiation adopted.

Accordingly, as a crosschecking, we have computed the hydrograph also using a 3D commercial code, which solves Reynolds equations using a biphasic volume of fluid technique (VOF) (Hirt and Nichols 1981). Fig. 5 shows that the 2D and 3D approaches are in good agreement also in the initial phase. This comparison also provides a confirmation that, as far as the discharge hydrograph is concerned, the differences related to a better description of the flow field around the breach are, from an engineering point of view, negligible. Similar conclusions have been obtained in the case of total dam break also by other writers (e.g., Mohapatra et al. 1999) who have shown that vertical acceleration affects only the first instants of the process. On the other hand, the computational burden implied by the two types of simulation is extremely different: the ratio of the computational times for the 3D and 2D simulations shown in Fig. 5 is approximately 10.

In order to test the effect of grid spacing Δx on the numerical solution, Fig. 6 shows the variation of the peak discharge for increasing $w/\Delta x$ (being w the breach width). As one can observe, a good convergence can be obtained for $w/\Delta x > 10$. This condition has been satisfied for all the simulations. Finally, it might be interesting to consider the effect of friction on the discharge hydrograph at the breach. Fig. 7 shows the hydrographs obtained for Manning's $n=0.0167$, 0.0125, 0.009, and 0 $m^{-1/3}$ s using a 2D and 3D approach, evidencing that friction plays a minor role on the initial phase of the emptying process. It does not affect the peak discharge but contributes to smoothen and extend the tail of the hydrograph. In particular, the simulation accomplished in smooth condition shows a wavy pattern along the tail that is a consequence of the propagation of negative waves within the reservoir and of their reflection on the upstream boundary and on the remaining part of the dam. These fluctuations are damped by resistance.

Synthesis of Numerical Results

In order to obtain a significant base of numerical results for testing the validity of Eq. (8), the De Saint Venant solver has been used to model the emptying process caused by a partial dam break in a reservoir whose geometry is described by Eq. (1). More than 200 different numerical cases have been considered for testing the conclusions of Section 2 and the corresponding 2D bathymetries have been described using digital elevation models with square cells of 1 m side.

To identify the range of variation of parameters δ, λ, and S_0 typical of real reservoirs, the topography of many mountain valleys located in the Italian Alps, eligible sites for potential reservoir construction, has been analyzed. Accordingly, the λ variation

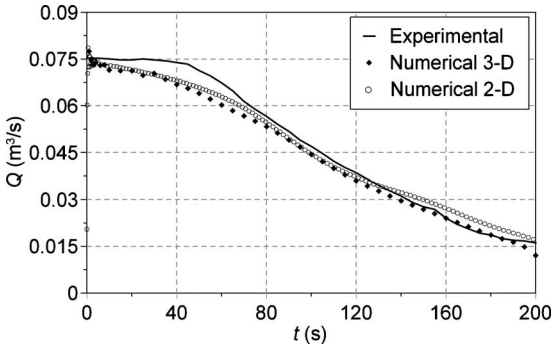

Fig. 5. Comparison between measured hydrograph (WES), MacCormack 2D, and VOF 3D simulations for a Manning's coefficient equal to 0.009 $m^{-1/3}$ s

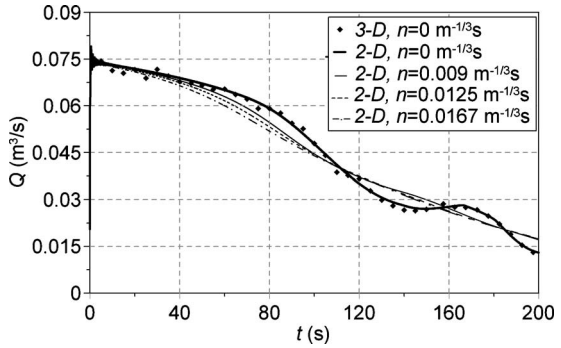

Fig. 7. Discharge hydrographs at the breach obtained from VOF 3D and MacCormack 2D simulations for different values of Manning's coefficient

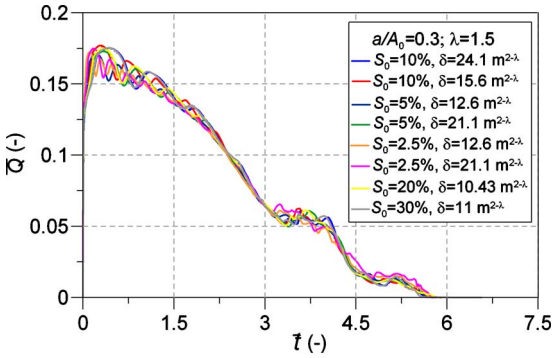

Fig. 8. Set of dimensionless hydrographs at the breach for different S_0 and δ values ($a/A_0=0.3$; $\lambda=1.5$)

range was found between 1.2 and 2 (see Fig. 2), whilst δ varies between 1 and 120 $m^{2-\lambda}$. As far as the slope S_0 is concerned, we have decided to consider a range between 1 and 30%, because higher slopes would imply severe limitations to the upstream stored volume (limiting the economic interest of the reservoir), and would violate one of the hypothesis at the basis of Eq. (9).

Within these parameter variation ranges, we have simulated sudden partial dam breaks with breach ratios $a/A_0=1$, $a/A_0=0.75$, $a/A_0=0.5$, $a/A_0=0.3$, and $a/A_0=0.25$, being $A_0=\delta h_0^{\lambda}$. Considering that the primary effect of resistance is detectable only on the tail of the discharge hydrograph and the difficulty of predicting the roughness of real reservoirs, the simulations have been accomplished in smooth condition.

All the breach hydrographs, which are the main results of the numerical simulations, when made dimensionless according to Eq. (8) for given values of λ and a/A_0, show a similar pattern, so confirming the conclusions of Section 2. An example is given by Fig. 8 where the symbols $\bar{Q}$ and $\bar{t}$ have been used respectively for the dimensionless discharge (Π_7) and time (Π_6) of Eq. (8).

The numerical results show that the dimensionless peak discharge $\overline{Q_p}$ is independent from λ, not only in the case of total dam break (as required by Su and Barnes' theoretical solution) but also when $a/A_0<1$, so confirming the effectiveness of the standardization given by Eq. (6). Accordingly, the peak discharge at the breach is essentially a function of $\Pi_2=a/A_0$ only and can be expressed as

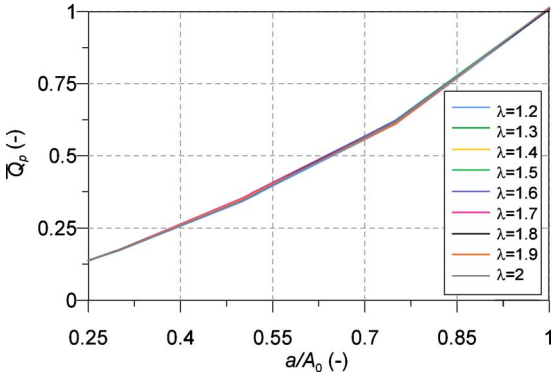

Fig. 9. Dimensionless peak discharge obtained by 2D simulations as a function of λ and of the breach ratio a/A_0

Table 1. Dimensionless Peak Discharge as a Function of the Breach Ratio a/A_0

Variable	Values				
a/A_0 (–)	1	0.75	0.5	0.3	0.25
k(–)	1	0.6173	0.3494	0.1743	0.1383

$$\overline{Q_p} \equiv \frac{Q_p}{\delta h_0^{\lambda}\sqrt{g h_0}}\left(\sqrt{\lambda}\left(\frac{2\lambda+1}{2\lambda}\right)^{2\lambda+1}\right)^{a/A_0} = k(a/A_0) \qquad (12)$$

where $k(a/A_0)$=a priori unknown function (that can be identified on the basis of the numerical results) and where $k(1)=1$ for consistency with Eq. (4). This is made evident by Fig. 9, where the average values of $\overline{Q_p}$, obtained by processing the ensemble of the dimensionless numerical hydrographs in correspondence of each $(\lambda, a/A_0)$ pair, are represented as a function of the breach ratio a/A_0 and, parametrically, of λ. All the lines corresponding to the different λ values tend to collapse into a single line. Their average values are listed in Table 1 and identify the unknown function $k(a/A_0)$ of Eq. (12). In a similar way, the average reservoir emptying time $\overline{t_f}$ has been obtained. These values are listed in Table 2 and graphically shown in Fig. 10.

Eq. (8) suggests and the numerical results confirm that when a/A_0 and λ are assigned all the hydrographs show a similar pattern (see Fig. 8). Accordingly, this pattern could be approximated by a single function that could be regarded as a synthetic dimensionless hydrograph. For simplicity, a polynomial model, whose coefficients can be easily determined on the basis of some simple conditions, has been considered. In particular, best results have been obtained with a fourth degree polynomial expression

$$\bar{Q}(\bar{t}) = \tfrac{1}{2}b_4\bar{t}^4 + \tfrac{1}{2}(b_3+c_3)\bar{t}^3 + \tfrac{1}{2}(b_2+c_2)\bar{t}^2 + \tfrac{1}{2}(b_1+c_1)\bar{t} + \tfrac{1}{2}(b_0+c_0) \qquad (13)$$

obtained as the average value of another fourth degree and third degree polynomial expressions

$$\bar{Q}(\bar{t}) = b_4\bar{t}^4 + b_3\bar{t}^3 + b_2\bar{t}^2 + b_1\bar{t} + b_0 \qquad (14)$$

$$\bar{Q}(\bar{t}) = c_3\bar{t}^3 + c_2\bar{t}^2 + c_1\bar{t} + c_0 \qquad (15)$$

The coefficients b_i, which identify Eq. (14), can be computed by imposing the following five conditions. First of all, although in reality the peak discharge of numerical hydrographs $\overline{Q_p}$ occurs very close but after the onset of the dam break, we have supposed that this value occurs instantaneously, by imposing

Table 2. Dimensionless Reservoir Emptying Time as a Function of λ and of the Breach Ratio a/A_0

	a/A_0				
λ	1	0.75	0.5	0.3	0.25
1.2	3.1030	3.0940	5.2477	8.9995	11.1671
1.3	3.0133	3.0027	4.2457	7.7418	9.8093
1.4	2.9262	2.9206	3.9010	6.6144	7.9905
1.5	2.8400	2.8341	3.6997	5.9528	7.2771
1.6	2.7699	2.7620	3.3281	5.5407	6.4967
1.7	2.7012	2.6945	3.1172	5.1902	5.7273
1.8	2.6276	2.6231	2.8326	4.8961	5.4531
1.9	2.5656	2.5566	2.7897	4.3643	5.2446
2	2.4997	2.4741	2.4819	3.9346	5.0603

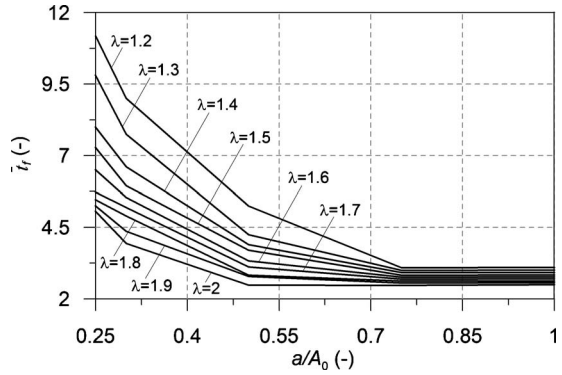

Fig. 10. Dimensionless reservoir emptying time obtained by 2D simulations as a function of λ and of the breach ratio a/A_0

1. $\bar{Q}=\overline{Q_p}$ when $\bar{t}=0$.
   The second condition is
2. $\partial\bar{Q}/\partial\bar{t}=0$ when $\bar{t}=0$.
   The third and fourth conditions are similar but referred to the reservoir emptying time $\bar{t}_f$, when the discharge tends to zero
3. $\bar{Q}=0$ when $\bar{t}=\bar{t}_f$.
4. $\partial\bar{Q}/\partial\bar{t}=0$ when $\bar{t}=\bar{t}_f$.
   The fifth condition is based on mass conservation. Let V_0 and $\bar{V}_0$ be the dimensional and dimensionless average volume initially stored within the reservoir

$$\bar{V}_0=\frac{V_0}{\delta h_0^{\lambda}}\left(\sqrt{\lambda}\left(\frac{2\lambda+1}{2\lambda}\right)^{2\lambda+1}\right)^{a/A_0}\frac{1}{\sqrt{\lambda}L_0} \tag{16}$$

   the final condition dictates that the integral of the polynomial expression is equal to the available volume
5. $\int_0^{\bar{t}_f}\bar{Q}(\bar{t})d\bar{t}=\overline{V_0}$.

By imposing these five constraints the linear system (17) can be easily obtained, whose solution is the set of coefficients b_i of Eq. (14)

$$\begin{cases} b_0=\overline{Q_p} \\ b_1=0 \\ b_4\bar{t}_f^4+b_3\bar{t}_f^3+b_2\bar{t}_f^2+b_1\bar{t}_f+b_0=0 \\ 4b_4\bar{t}_f^3+3b_3\bar{t}_f^2+2b_2\bar{t}_f+b_1=0 \\ \frac{1}{5}b_4\bar{t}_f^5+\frac{1}{4}b_3\bar{t}_f^4+\frac{1}{3}b_2\bar{t}_f^3+\frac{1}{2}b_1\bar{t}_f^2+b_0\bar{t}_f=\overline{V_0} \end{cases} \tag{17}$$

The other set of coefficients c_i for Eq. (15) is computed by imposing constraints 1, 3, 4, and 5, so obtaining the system

$$\begin{cases} c_0=\overline{Q_p} \\ c_3\bar{t}_f^3+c_2\bar{t}_f^2+c_1\bar{t}_f+c_0=0 \\ 3c_3\bar{t}_f^2+2c_2\bar{t}_f+c_1=0 \\ \frac{1}{4}c_3\bar{t}_f^4+\frac{1}{3}c_2\bar{t}_f^3+\frac{1}{2}c_1\bar{t}_f^2+c_0\bar{t}_f=\overline{V_0} \end{cases} \tag{18}$$

It is relevant to observe that the two simplified hydrographs provided by the third and fourth order polynomials are usually very similar, like in the case shown in Fig. 14, where the three polynomials in Eqs. (13)–(15) are plotted versus experimental results. In other cases, the advantage provided by one of two polynomials in Eqs. (14) and (15) is more evident, being difficult, however, to identify a priori which one performs better. Accordingly, with the aim of providing a general simplified procedure, the overall best results have empirically been obtained by using an average of the two polynomials.

Fig. 11 presents, for two different values of λ, a comparison between the five variation bands of hydrographs obtained by 2D numerical simulation for $a/A_0=1$, 0.75, 0.5, 0.3, 0.25, and the polynomial-model hydrographs Eq. (13). Each variation band has been built by considering, for each value of the dimensionless time, the minimum and the maximum dimensionless discharge observed in the numerical hydrographs at fixed a/A_0. In order to make each figure more easily readable, we plotted the hydrographs according to the dimensionless discharge

$$\overline{Q'}\equiv\frac{Q}{\delta h_0^{\lambda}\sqrt{gh_0}}\sqrt{\lambda} \tag{19}$$

in place of expression (6). Actually, expression (6) would imply that $\bar{Q}=1$ when $\bar{t}=0$, irrespective of λ and a/A_0, so that all the hydrographs in Fig. 11 corresponding to different values of a/A_0 would tend to merge together in the region around the peak, making very difficult their intercomparison. If λ is assigned, expression (19) and (6) differ only for a scaling factor that is a function of a/A_0.

Fig. 11 suggests two general observations. First, the width of each variation band is always rather small, so confirming the validity of Eq. (8). In addition, the polynomial hydrograph Eq. (13) provides a very good approximation to the average trend within each band.

Identification of a Simplified Methodology to Characterize the Hydrograph Following a Sudden Partial Dam Break

Whilst it is required that the reservoir bathymetry reasonably complies with the geometrical hypothesis which are at the basis

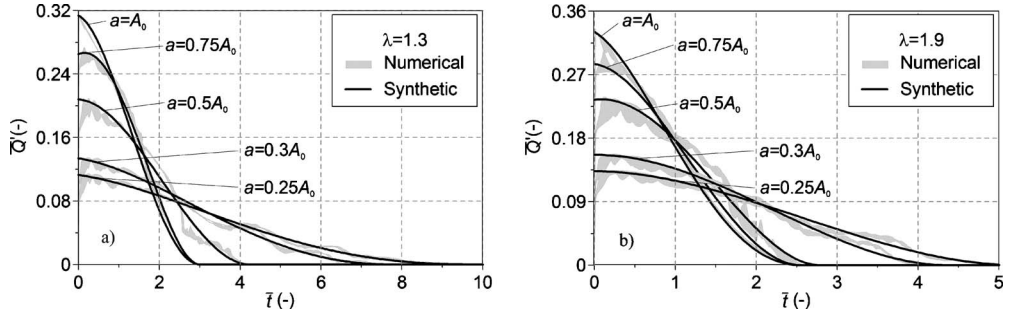

Fig. 11. Comparison between the numerical set of dimensionless hydrographs and their polynomial approximations for different a/A_0 values: (a) λ=1.3; (b) λ=1.9

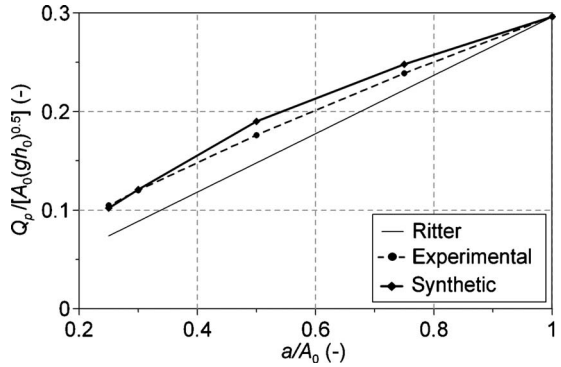

Fig. 12. Comparison between measured (WES) and computed dimensionless peak discharge as a function of the breach ratio a/A_0

of the proposed procedure, the only information that is required for the application of this methodology is the stage-volume relationship, the initial water depth h_0 within the reservoir and the corresponding wetted area at the dam cross section, A_0. Finally, one must know the area a of the breach, in order to establish the corresponding ratio a/A_0.

The identification of the hydrograph at the dam section following a sudden and partial collapse can be accomplished by following a few simple steps:

1. First of all, it is straightforward to show that the volume initially stored within a reservoir like the one shown in Fig. 1 is given by

$$V_0 = \int_{h_0}^{0} -\frac{\delta h^{\lambda}}{S_0} dh = \frac{\delta}{S_0(\lambda+1)} h_0^{\lambda+1} \tag{20}$$

accordingly, the stage-volume curve is

$$V(h) = \frac{\delta}{S_0(\lambda+1)} h^{\lambda+1} = \eta h^{\lambda+1} \tag{21}$$

On the basis of the real stage-volume curve the two parameters λ and η can be easily obtained by a least squares approximation.

2. By considering the initial wetted area at the dam cross section, A_0, and the computed λ value, Eq. (1) immediately provides δ. By substitution in Eq. (21), the equivalent slope S_0 of the reservoir thalweg can be computed.
3. By using the selected a/A_0 ratio, the discharge Q_0

$$Q_0 = \delta h_0^{\lambda} \sqrt{g h_0} \left(\frac{1}{\sqrt{\lambda}} \left(\frac{2\lambda}{2\lambda+1} \right)^{2\lambda+1} \right)^{a/A_0} \tag{22}$$

and the time t_0

$$t_0 = \sqrt{\frac{h_0 \lambda}{g}} \frac{L_0}{h_0} \tag{23}$$

needed to compute dimensionless time and discharge according to Eq. (8), can be obtained.

4. By linear interpolation of the data in Tables 1 and 2 (otherwise by Figs. 9 and 10), the value of $\overline{Q_p}$ and $\overline{t_f}$ can be obtained. The value of the dimensionless volume $\bar{V}_0$ has to be calculated by dividing the initially stored volume within the reservoir, V_0, by the product between Q_0 and t_0 [Eq. (16)]. Here the value V_0 is provided by the real stage-volume curve.
5. Systems (17) and (18) can now be solved to obtain the parameters of the dimensionless polynomial hydrograph Eq. (13). It is now straightforward to derive the dimensional simplified hydrograph $Q(t)$.

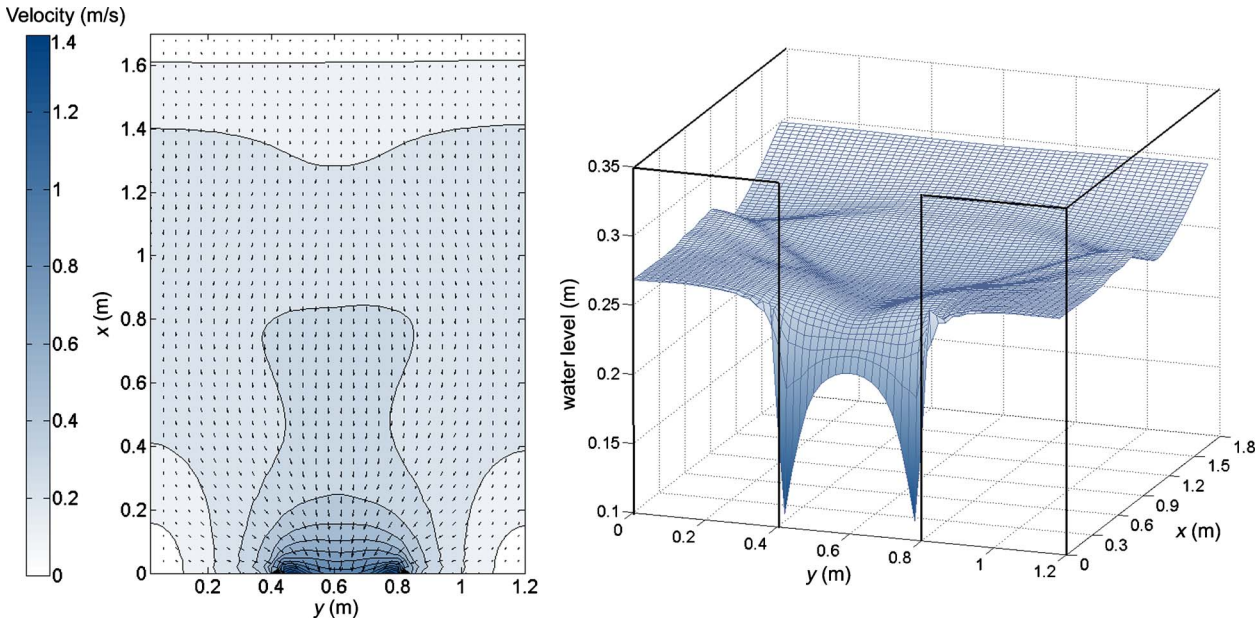

Fig. 13. Convergence of the flow field around the breach at $t=1$ s after the dam break

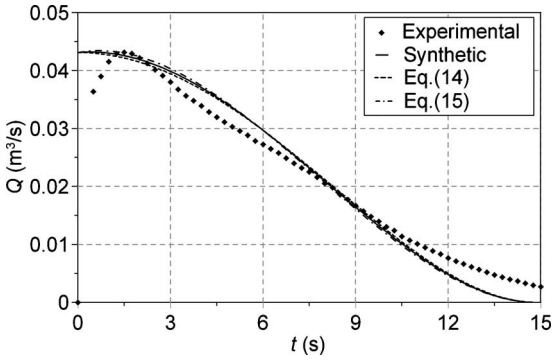

Fig. 14. Measured (Chervet and Dallèves 1970) and simplified discharge hydrographs at the breach

Discussing the Proposed Procedure and Testing Its Predictive Capability

Considering that it is extremely difficult to provide an accurate measurement of the discharge hydrograph following a real dam break case, in order to test the effectiveness of the proposed approach, one can resort only to laboratory results. The WES set of hydrographs cannot be used because derived in a channel having a slope (0.005 m/m) that is 1/2 than the minimum one explored in this paper. However, the data regarding the peak discharge can be used for the validation because they are largely unaffected by channel slope and roughness. On the basis of its experiments Schoklitsch (1917) proposed the following equation for peak discharge in the case of the full depth partial width breaches in rectangular channel:

$$\frac{Q_p}{A_0\sqrt{gh_0}} = \frac{8}{27}\left(\frac{a}{A_0}\right)^{3/4} \tag{24}$$

This equation was confirmed by WES (1960) and can be compared with the more general Eq. (12). Although the rectangular case is outside of the numerical field of investigation explored in our work ($1.2 \leqslant \lambda \leqslant 2$), the dimensionless peak discharge $\overline{Q_p}$ given by Eq. (12) is practically independent from λ (see Fig. 9). Accordingly, it seems legitimate to apply Eq. (12) also for rectangular cross section ($\lambda = 1$). In this case, Eq. (12) can be written as

$$\frac{Q_p}{A_0\sqrt{gh_0}} = k(a/A_0)\left(\frac{8}{27}\right)^{a/A_0} \tag{25}$$

where $k(a/A_0)$ values are given in Table 1. Eqs. (24) and (25) are plotted in Fig. 12 as a function of the a/A_0 ratios of Table 1, clearly evidencing a satisfactory agreement, with an average percentage difference of 3.0 and a maximum of 7.9. A feature of Eqs. (12) and (24) that can be observed in Fig. 12 is that the peak discharge is higher than the value one would obtain from the application of Ritter's solution (shown as a third curve in Fig. 12) computed considering the breach area a. Actually, the discharge provided by Ritter's solution represents the discharge at the very onset of the dam break process. The discharge hydrograph peak, however, is located later and is caused by the complex pattern of the water surface drawdown in the area surrounding the breach, as can be appreciated in Fig. 13 for the WES (3.1) test case.

Another validation of the proposed simplified procedure involving also the shape of the hydrograph can be accomplished using the experimental data of Chervet and Dallèves (1970) regarding a dam break in a sloping rectangular channel, with $S_0 = 0.04$ m/m and $a/A_0 = 1$. Channel width and initial water depth behind the dam are 0.3 m, the channel Manning's n is 0.014 s/m$^{1/3}$. Fig. 14 shows the comparison between the experimental data and the hydrograph that can be obtained by applying the proposed procedure, although assuming $\lambda = 1.2$, that is the value in Table 2 closest to the experimental situation. Actually, contrary to the dimensionless peak discharge, the dimensionless reservoir emptying time, that is needed for the construction of the hydrograph, strongly depends on λ. Nevertheless there is a good agreement between the two hydrographs, although the tail of the simplified hydrograph is shorter than the experimental one. This effect, of limited interest from the practical point of view, is very likely related both to the mismatch between real and simulated λ and to channel resistance.

In order to further verify the effectiveness of the proposed procedure an extensive set of tests using real bathymetries was carried out. For each case, the polynomial expression Eq. (13) was compared with the numerical hydrograph obtained at the breach section by solving the 2D De Saint Venant equations [Eq. (9)]. These equations are widely accepted in the literature as the state-of-the-art tool for the accurate reconstruction of complex dam break scenarios (e.g., Valiani et al. 2002; Begnudelli and

Table 3. Characteristics of the Reservoirs Considered in This Study

Reservoir	V_0 (m^3)	h_0 (m)	A_0 (m^2)	a/A_0 (–)	λ (–)	η ($m^{4-\lambda}$)	δ ($m^{2-\lambda}$)	L_0 (m)	S_0 (–)
Ridanna1	106,102,099	291	131,778	0.39	1.8	11.99	4.58	2,146.1	0.136
Ridanna2	74,032,899	198	70,775	0.38	1.7	45	8.57	2,816.7	0.07
Ridanna3	31,236,399	181	52,010	0.37	1.8	15	4.34	1,756.8	0.103
Valsesia1	35,158,098	160	41,068.4	0.3	1.76	28.864	5.42	2,352.5	0.068
Valsesia2	46,466,199	203	88,554.8	0.37	1.5	78	30.12	1,315.7	0.154
Valsesia3	46,878,299	187	53,953.06	0.39	1.67	39.99	8.77	2,273.4	0.082
Valsesia4	86,204,198	220	79,609.8	0.43	1.82	2.56	4.35	3,071.3	0.072
Valsesia5	10,146,999	125	34,841	0.49	1.71	19.99	9.04	749.3	0.166
Adamé	4,697,624	31.793	5,273.98	0.4/0.7	1.66	499.999	16.57	2,557.2	0.012
Valtellina1	920,671.5	44.23	3,148.16	0.37	1.78	23.79	3.62	809.6	0.055
Valtellina2	1,564,298.4	30.796	3,009.35	0.35	1.49	309.62	17.89	1,329.4	0.023
Valtellina3	896,576.6	57.82	7,663.44	0.37	1.7	15.07	7.68	306.57	0.188
Brembo	16,266,345	137.4	25,989.38	0.32	1.9	9.99	2.2988	1,740.28	0.079

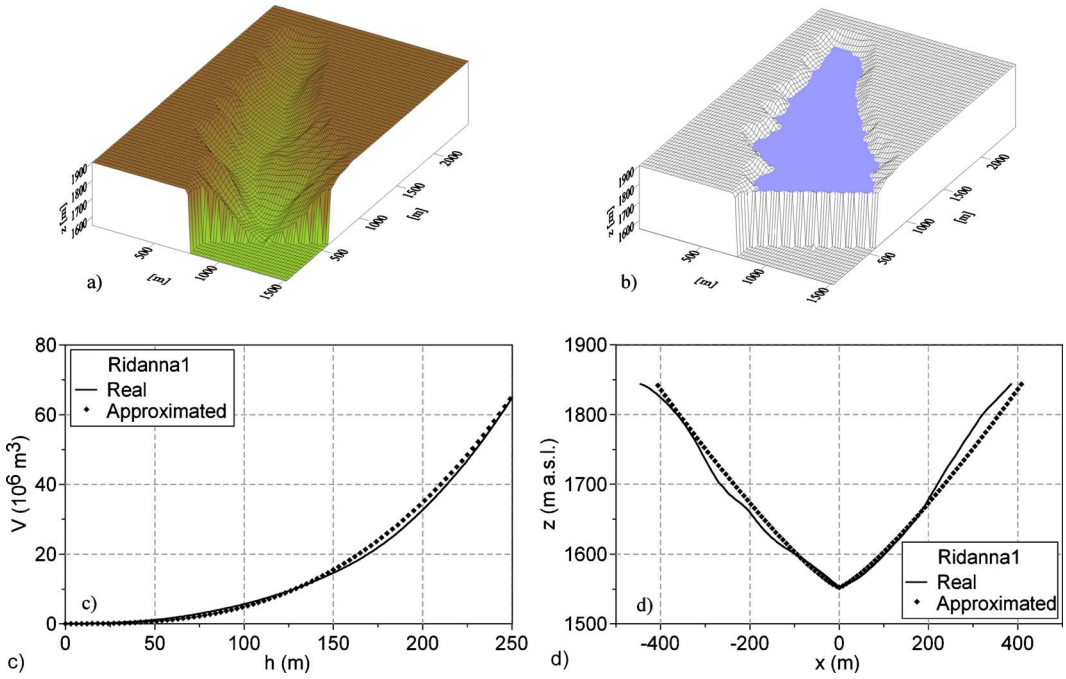

Fig. 15. Geometrical characteristics of the Ridanna1 basin: (a) 3D view of the bathymetry; (b) 3D view of the water surface within the reservoir before the failure; (c) real storage-depth curve [Eq. (21)] compared to the fitted one; and (d) real and approximated [Eq. (1)] cross sections at the dam location

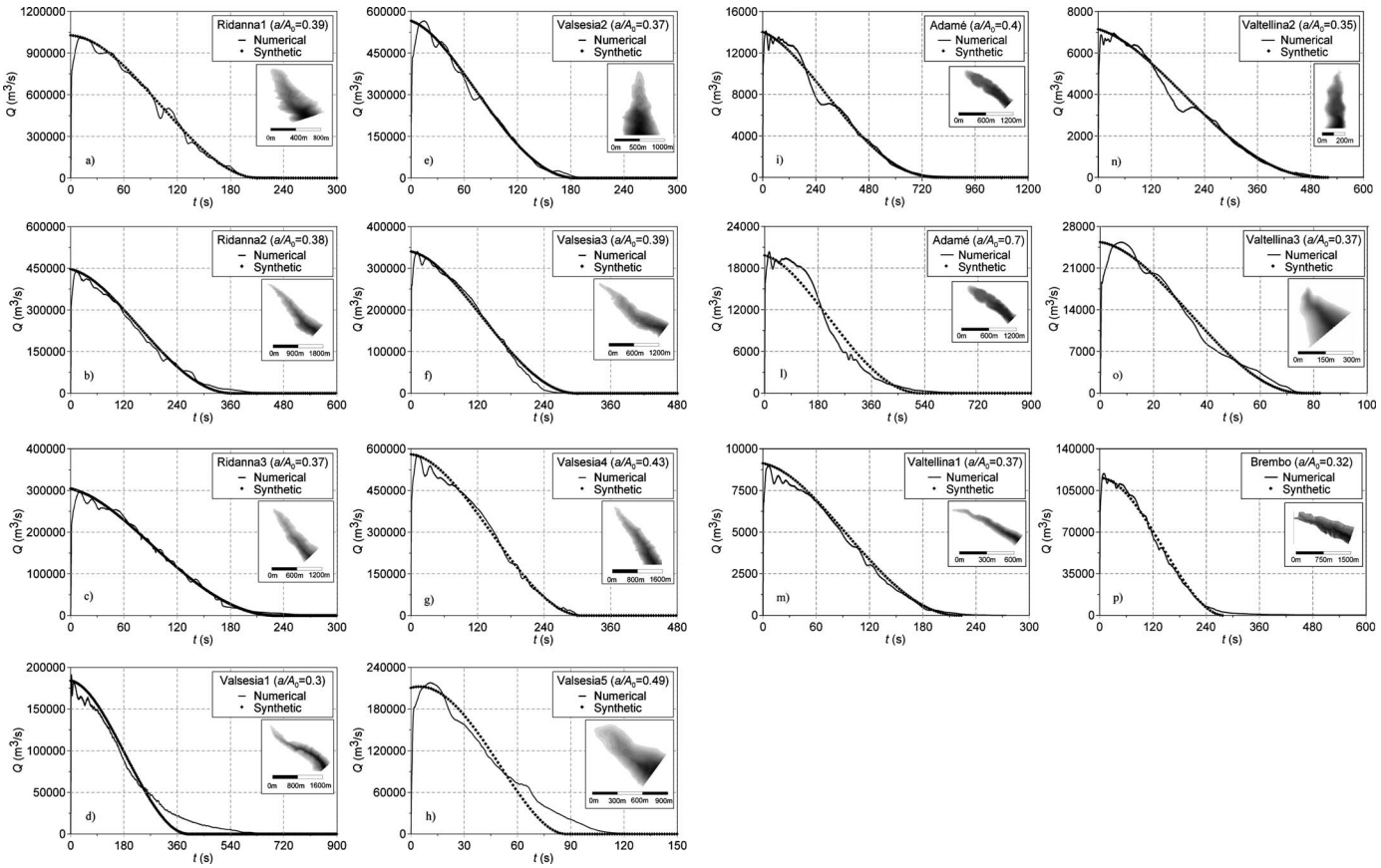

Fig. 16. Comparison between computed and simplified hydrographs for the considered real bathymetries

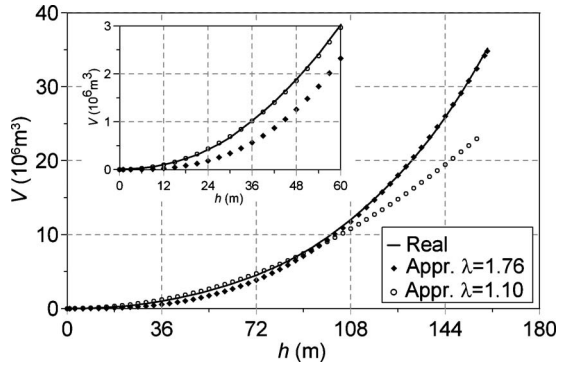

Fig. 17. Valsesia1 stage-volume curve and two least square approximations, corresponding to $\lambda=1.76$ and $\lambda=1.1$

Sanders 2007; CADAM and IMPACT projects: Soares Frazão et al. 2000; Soares Frazão et al. 2003).

To this purpose, a numerical description of the bathymetry is obviously required, a piece of information that is not always available. Accordingly, in order to get a large testing set, both the bathymetry and the stage-volume curve were derived on the basis of the digital elevation model (DEM) for a group of alpine valleys which potentially could have been the location of real reservoirs. The DEM space discretization varies between 5 and 20 m. Most of the simulations were done using a breach ratio a/A_0 close to 1/3, as assumed in a previous section. Overall, 13 different reservoirs were considered, in order to explore a wide range of reservoir volumes, stages, slopes and shape parameters, as shown in Table 3. Actually, different combinations of these parameters can significantly influence the characteristics of the emptying process.

In order to make our comparison as complete as possible, it would be necessary to compare graphically the real and the approximated stage-volume curve Eq. (21), the real cross section at the dam location and the corresponding approximation Eq. (1), and, last but most important, the numerically computed hydrograph and the simplified one, Eq. (13). Due to space constraints, this detailed presentation will be limited to the first case (Ridanna1, see Fig. 15). Only the comparison between the hydrographs will be shown for the other ones in Fig. 16. In general, one can observe a good agreement although in some cases (i.e., Valsesia1 and Valsesia5) the synthetic hydrograph provides a shorter tail than the one turning out from the 2D simulation. This mismatch, rather irrelevant from the practical point of view, is related to the vertical mass distribution within the reservoir and can be appreciated considering its stage-volume curve. The least squares approximation that gives the two parameters λ and η in Eq. (21) should provide an overall good approximation of the stage-volume curve. If this is not possible, the emphasis of the fitting process should be put on the part of the curve corresponding to the highest stages, which govern the initial, most important part of the hydrograph. In this case, however, one might expect a mismatch in the hydrograph tail. This situation is portrayed in Fig. 17, where the stage-volume curve for Valsesia1 is shown along with two least square approximations. The first approximation, corresponding to $\lambda=1.76$, has been computed using all the data. The second one has been calibrated with stages lower than 80 m, and clearly shows (see inset of Fig. 17) that a better approximation at low stages is provided by $\lambda=1.1$. Since it is an easy task to show that the lower the exponent of the stage-volume curve, the longer the tail (see e.g., Macchione and Rino 2008), the approximation using $\lambda=1.76$ provides an overall good response with the exception of the final part of the emptying process, where a lower value of λ would provide a better reconstruction.

Conclusions

In this contribution, a simple procedure to identify, in an effective way, the hydrograph following a sudden partial dam break has been proposed, under the hypothesis that the valley containing the reservoir can be assumed as prismatic with a monomial cross section, according to Su and Barnes' classical description Eq. (1). Exploring a wide range of the geometric parameters and on the basis of an extensive set of numerical simulations of 2D De Saint Venant equations, a suitable adimensionalization of the numerical results has been proposed. This procedure leads to a description of the breach hydrograph in terms of a biunique relationship between dimensionless discharge and dimensionless time for assigned breach ratio a/A_0 and shape parameter λ. This hydrograph can be approximately described by a fourth degree polynomial expression that is identified by a set of simple geometrical and physical constraints. This description can be effectively used with real reservoirs for which the actual volume-depth curve and area A_0 of the dam cross section in correspondence of the initial water depth h_0 are known. In this case, by solving two linear systems, the dimensionless hydrograph in correspondence of a selected breach area a can be obtained in a straightforward way. The proposed approach is extremely simple and demands very few information that is usually available for all reservoirs. It has been proven effective in representing in a careful way the hydrographs calculated through 2D simulations of the emptying process following a sudden partial dam break in real bathymetries. A code implementing the presented algorithm is freely available upon request to the writers.

Acknowledgments

We wish to thank the reviewers and the editor, whose comments contributed to improve the quality of this paper.

Notation

The following symbols are used in this paper:

A = wetted area in correspondence of depth h;
A_0 = wetted area at the dam in correspondence of depth h_0;
a = area of the partial breach in correspondence of depth h_0;
B = free-surface width in correspondence of depth h;
b_i, c_i = coefficients of ith power terms in Eqs. (14) and (15);
E, F = flux vectors along x- and y-directions in 2D De Saint Venant equations;
g = acceleration due to gravity;
h = water depth;
h_0 = initial water depth at the dam;
L_0 = initial extent of the water surface, measured orthogonally to the dam;
n = Manning's roughness coefficient;
Q = discharge;
Q_p = peak discharge;
Q_0 = reference discharge [Eq. (22)];

$\bar{Q}$ = dimensionless discharge, coincident with Π_7 [Eq. (6)];
$\overline{Q_p}$ = dimensionless peak discharge [Eq. (12)];
$\overline{Q'}$ = dimensionless discharge [Eq. (19)];
S = vector of source terms in 2D De Saint Venant equations;
S_{fx}, S_{fx} = slope friction along x- and y-directions;
S_0 = bottom slope;
S_{0x}, S_{0x} = bottom slope along x- and y-directions;
t = time;
t_0 = reference time [Eq. (23)];
$\bar{t}$ = dimensionless time, coincident with Π_6 [Eq. (3)];
$\overline{t_f}$ = dimensionless emptying time of the reservoir;
U = vector of conserved variables in 2D De Saint Venant equations;
u, v = flow velocity components along x- and y-directions;
V = volume within the reservoir in correspondence of depth h;
V_0 = volume initially stored within the reservoir;
$\bar{V}_0$ = dimensionless volume initially stored within the reservoir;
w = width of partial breach;
χ = Chezy's coefficient;
x, y = orthogonal space coordinates in the horizontal plane;
z = bottom elevation;
Δx = numerical grid spacing;
δ = coefficient of the power law expressing wetted area as a function of depth [Eq. (1)];
η = coefficient of the power law expressing the stage-volume curve of the reservoir [Eq. (21)];
λ = exponent of the power law expressing wetted area as a function of depth [Eq. (1)]; and
Π_i = ith dimensionless group.

References

Alcrudo, F., and Garcia Navarro, P. (1993). "A high resolution Godunov type scheme in finite volumes for the 2D shallow water equation." *Int. J. Numer. Methods Fluids*, 16, 489–505.

Aureli, F., Maranzoni, A., Mignosa, P., and Ziveri, C. (2007). "A simple methodology for the dam-break wave evaluation." *Proc., 32nd Congress of IAHR* (CD-ROM), Corila, Venice.

Bazin, H. (1865). "Recherches Expérimentales relatives aux remous et à la propagation des ondes [Experimental research on the hydraulic jump and on wave propagation]." *Deuxième partie des Recherches hydrauliques de Darcy et Bazin*, Dunod, Paris, 148.

Begnudelli, L., and Sanders, B. F. (2007). "Simulation of the St. Francis dam-break flood." *J. Eng. Mech.*, 133(11), 1200–1212.

Bukreev, V. (2006). "On the discharge characteristic at the dam site after dam break." *J. Appl. Mech. Tech. Phys.*, 47(5), 679–687.

Chervet, A., and Dallèves, P. (1970). "Calcul de l'onde de submersion consécutive à la rupture d'un barrage [Computation of the flooding wave following a dam break]." *Schweizerische Bauzeitung*, 88(19), 420–432.

Dressler, R. F. (1958). "Unsteady non-linear waves in sloping channels." *Proc. R. Soc. London, Ser. A*, 247(1249), 186–198.

Fennema, R. J., and Chaudhry, M. H. (1990). "Explicit methods for 2-D transient free surface flows." *J. Hydraul. Eng.*, 116(8), 1013–1034.

Goubet, A. (1979). "Risques associés aux barrages [Dam related risks]." *Houille Blanche*, 8, 475–490.

Hirt, C. W., and Nichols, B. D. (1981). "Volume of fluid (VOF) method for the dynamics of free boundaries." *J. Comput. Phys.*, 39, 201–225.

ICOLD. (1998). "Dam-break flood analysis—Review and recommendations." *Bulletin 111*.

Macchione, F., and Rino, A. (2008). "Model for predicting floods due to earthen dam breaching. II: comparison with other methods and predictive use." *J. Hydraul. Eng.*, 134(12), 1697–1707.

Mohapatra, P. K., Eswaran, V., and Murty Bhallamudi, S. (1999). "Two-dimensional analysis of dam-break flow in vertical plane." *J. Hydraul. Eng.*, 125(2), 183–192.

Owen, H. J. (1980). *Flood emergency plans: Guidelines for corps dams*, Hydrologic Engineering Center, Davis, CA.

Pilotti, M., Maranzoni, A., and Tomirotti, M. (2006). "Modellazione matematica della propagazione dell'onda di piena conseguente al crollo della diga del Gleno [Mathematical modeling of the Gleno dam break wave]." *Proc., XXX Convegno di Idraulica e Costruzioni Idrauliche* (CD-ROM), Università La Sapienza, Rome.

Ritter, A. (1892). "Die Fortpflanzung der Wasserwellen [The propagation of water waves]." *Zeitschrift des Vereines Deutscher Ingenieure*, 36(33), 947–954.

Sakkas, J. G., and Strelkoff, T. (1973). "Dam-break flood in a prismatic dry channel." *J. Hydraul. Div.*, 99(12), 2195–2216.

Schoklitsch, A. (1917). "Über Dammbruchwellen [On waves created by dam breaches]." *Sitzungberichten der Kaiserliche Akademie der Wissenschaften in Wien*, 126, 1489–1514.

Soares Frazão, S., Morris, M. W., and Zech, Y. (2000). *Concerted action on dambreak modelling: Objectives, project report, test cases, meeting proceedings* (CD-ROM), Université Catholique de Louvain, Civ. Eng. Dept., Hydraulics Div., Louvain-la-Neuve, Belgium.

Soares Frazão, S., Zech, Y., and Morris, M. (2003). "IMPACT, Investigation of extreme flood processes and uncertainty." *Proc., 3rd Project Workshop* (CD-ROM).

Su, S. T., and Barnes, H. (1970). "Geometric and frictional effects on sudden releases." *J. Hydraul. Div.*, 96(11), 2185–2200.

U.S. Army Corps of Engineers (USACE). (1997). "Engineering and design. Hydrologic engineering requirements for reservoirs." *Engineer manual 1110-2-1420*, Washington, D.C.

Valiani, A., Caleffi, V., and Zanni, A. (2002). "Case study: Malpasset dam-break simulation using a 2D finite volume method." *J. Hydraul. Eng.*, 128(5), 460–472.

Waterways Experiment Station (WES). (1960). "Floods resulting from suddenly breached dams. Misc paper no 2-374. Rep 1: Conditions of minimum resistance." *Rep. Prepared for U.S. Army Corps of Engineers*, Vicksburg, MS.

Wu, C., Huang, G., and Zheng, Y. (1999). "Theoretical solution of dam-break shock wave." *J. Hydraul. Eng.*, 125(11), 1210–1215.